Journal of Hydrology 530 (2015) 580–590

Contents lists available at ScienceDirect

Journal of Hydrology

journal homepage: www.elsevier.com/locate/jhydrol

Area representative soil water content estimations from limited measurements at time-stable locations or depths

Dongli She [a,b,*], Wenjuan Zhang [a], Jan W. Hopmans [c], Luis Carlos Timm [d]

[a] Key Laboratory of Efficient Irrigation-Drainage and Agricultural Soil-Water Environment in Southern China, Ministry of Education, College of Water Conservancy and Hydropower Engineering, Hohai University, Nanjing 210098, China
[b] State Key Laboratory of Soil and Sustainable Agriculture, Institute of Soil Science, Chinese Academy of Sciences, Nanjing 210008, China
[c] Department of Land, Air, and Water Resources, University of California, Davis, CA 95616, USA
[d] Faculty of Agronomy, Federal University of Pelotas, Department of Rural Engineering, P.O. Box 354, 96001-970 Pelotas, RS, Brazil

ARTICLE INFO

Article history:
Received 3 June 2015
Received in revised form 27 August 2015
Accepted 5 October 2015
Available online 13 October 2015
This manuscript was handled by Corrado Corradini, Editor-in-Chief, with the assistance of Renato Morbidelli, Associate Editor

Keywords:
Root-zone soil water
Time stability
Sampling schemes

SUMMARY

To minimize the number of soil water content (*SWC*) measurements for estimation of field- or watershed-scale soil water storage, we present an analysis of time-stable soil water data across both measurement locations and soil depth intervals. The proposed analysis applies the time stability concept to select area-representative measurement locations, and assesses the potential for identifying the most time-stable depth interval (MTSD) using a minimal number of selected time-stable locations (MTSLs). For that purpose, we used a time series of 21 *SWC* datasets, measured at 20 locations and 20 corresponding depth intervals down a 3-m soil profile, during a two-year period in the 38-ha study area of the Liudaogou watershed of the China Loess Plateau. After identifying the MTSLs, analysis of time stability of measurement depth intervals showed single soil water depth measurements at between 2 and 5 of the MTSLs were sufficient to determine the area-representative *SWC*. The MTSD was determined to be about midway in the soil profile, irrespective of total soil profile depth measured. Confirmation of the time-stability analyses was done by comparing the representative *SWC* estimations for the 38-ha sampling area with additional *SWC* measurements across the 6.9 km^2 watershed. The encouraging results of our analysis suggest that time stability analysis may be an effective way to assess large-scale soil water storage in arid and semi-arid regions.

© 2015 Elsevier B.V. All rights reserved.

1. Introduction

Soil water, sometimes referred to as green water, comprises a significant fraction of all available fresh water, as opposed to salt water, at the global scale (National Geographic Society, 2010; She et al., 2014a). Knowledge of root-zone soil water distribution is important when estimating plant available water, analyzing soil biochemical processes as controlled by water and temperature conditions, and scheduling irrigation, as well as when defining the land surface boundary conditions in climate models (Vereecken et al., 2008). However, information about soil water content (*SWC*) at the landscape scale is difficult to obtain (Vereecken et al., 2008; Hu et al., 2012; She et al., 2014b), especially as typically *SWC* is extremely variable, both in space and time. Consequently, there is great interest in optimizing soil water information, in terms of both measurement types and analyses (Hu et al., 2010; She et al., 2013). Recently, an entire issue of the Journal of Hydrology was devoted to examining some of these approaches across different spatial scales (Corradini, 2014). In the context of the presented study, we reviewed the literature that seeks to relate point to area-mean *SWC* values, specifically by analyzing *SWC* time stability (Vachaud et al., 1985; Heathman et al., 2003; She et al., 2014c).

The time-stability concept assumes that a limited number of point locations have the capacity to maintain a property value, such as *SWC*, in such a way as to represent the area-mean and extreme values of that property over time (Vachaud et al., 1985; Rolston et al., 1991). Consequently, the relative deviation between the time-stable measurement locations and field-averaged properties, or Mean Relative Difference (MRD) is time-independent. This concept has been extensively applied to the upscaling of point *SWC* measurements toward field-mean soil water storage conditions (Grayson and Western, 1998; She et al., 2012; Hu and Si, 2014). Based on time-stability analysis, studies have successfully used the measured *SWC* at time-stable locations to estimate the mean

* Corresponding author at: Key Laboratory of Efficient Irrigation-Drainage and Agricultural Soil-Water Environment in Southern China, Ministry of Education, Hohai University, Nanjing 210098, China. Tel.: +86 15996239659.
E-mail address: shedongli@hhu.edu.cn (D. She).

http://dx.doi.org/10.1016/j.jhydrol.2015.10.016
0022-1694/© 2015 Elsevier B.V. All rights reserved.

SWC of a larger area (Grayson and Western, 1998; She et al., 2012; Hu and Si, 2014) or across areas with no or limited soil water data being available (Parajka et al., 2005; Gao et al., 2013). Such time-stability analyses have been carried out at different scales: Vereecken et al. (2014) reviewed studies carried out at the field scale, while Liu and Shao (2014) considered a hillslope under four land use types and Molina et al. (2014) investigated a small abandoned agricultural Mediterranean terrace, and Zucco et al. (2014) studied soil spatial and temporal dynamics at the small (6 km^2) catchment scale. These analyses focused on the minimum number of time-stable locations required to optimize *SWC* prediction. Moreover, those time-stable locations with near-zero MRD values were considered to directly estimate the areal mean *SWC*, whereas otherwise the distribution of time-independent MRD can be used to characterize field soil variability in *SWC* (Grayson and Western, 1998). Estimation errors varied with estimation models that involved different time-stable locations (Mohanty and Skaggs, 2001). The time-stable locations with MRD values below zero typically underestimate the area-mean *SWC* value, while those larger than zero are overestimations (Vachaud et al., 1985). The estimation accuracy is increased by incorporating additional time-stable locations into the area-mean estimation models. However, additional *SWC* measurements are time-consuming or expensive to carry out (Gómez-Plaza et al., 2000; Xia et al., 2014). Therefore, there needs to be a trade-off between estimation accuracy and measurement costs. Most studies to date on time stability analysis of soil water focused on surface soil water (Grayson and Western, 1998; Gómez-Plaza et al., 2000; Brocca et al., 2008), with relatively few studies applied to deeper soil profiles (Gao and Shao, 2012; She et al., 2012), as such data are relatively limited.

In addition, the vertical *SWC* distribution in a soil profile may exhibit temporal stability, although depth variations are largely controlled by soil heterogeneity and root water uptake distribution (Gao and Shao, 2012; She et al., 2012). Therefore, in this study, we hypothesize that a combination of time-stability analyses in both the lateral (i.e., horizontal) and depth (i.e., vertical) directions to determine the corresponding most time-stable location (MTSL) and depth interval (MTSD) that can be used to upscale *SWC* indirectly. This would be especially meaningful for *SWC* evaluations at depths where it is more difficult to obtain *SWC* data (Hu et al., 2010). The objectives of this study are to: (1) analyze the upscaled *SWC* accuracy of using both profile *SWC* measurements and MTSD *SWC* measurements from one or more MTSL; and (2) to determine the optimum number of MTSLs for estimation of area-mean *SWC* using the MTSD measurements.

2. Materials and methods

2.1. Study site

A range of field-scale measurements were conducted in the Liudaogou watershed located in the north of the Loess Plateau of China (Latitude 35°20′–40°10′N; Longitude 110°21′–110°23′E) (Fig. 1). The watershed has an area of 6.9 km^2 and the elevation ranges between 1094 and 1274 m. The region is dominated by a cold semiarid climate with a mean daily temperature of 8.4 °C. The total annual rainfall ranges between 109 and 891 mm with a mean value of 437 mm, about 70% of which falls between June and September. The annual potential evapotranspiration is 785.4 mm, and the desiccation degree is 1.8. The dominant soil type in the watershed is a loessal mein soil (Calcaric Regosol, FAO/UNESCO, 1988), with the occasional presence of red loessal soil (Eutric Regosol), aeolian sand soil (Calcaric Arenosol), and soil deposits in terraced fields (Calcaric Fluvisol). Additional details about the watershed have been given in She et al. (2010, 2013).

2.2. Experimental design

The study area (38 ha; 1101–1187 m above sea level) was located in the south of the Liudaogou watershed, and was designated as Area A (Fig. 1). The soil type is a loess soil that is high in silt content (48.3%) and has a range of clay and sand contents that comprise 51.7% of the particle size distributions. Twenty soil profile water content measurement locations were randomly selected (P1 through P20). Each of the 20 measurement locations included 3 neutron probe access tubes, representing an area of about 5.0 m × 20.0 m. During the study period between 26 May 2007 and 11 October 2008, 21 determinations of *SWC* were made at irregular time intervals for each access tube. The *SWC* was determined depth intervals of 0.1 m for the 0.0–1.0 m soil profile, and at 0.2-m intervals for the 3.0 m soil profiles (i.e., a total of 20 measurement depth intervals). Volumetric soil water content values (*SWC*, %) at each depth were calculated from the neutron counting rate using the calibration curves shown in Fig. 2 and originally reported in She et al. (2014a), resulting in *SWC* measurement uncertainties of about 0.05 (shallow soil depths) to 0.03 $cm^3\ cm^{-3}$ (below 0.2 m). For each location (P1–P20), the three *SWC* measurements were averaged to represent each depth interval at each location. The mean soil profile *SWC* was calculated based on these averaged depth intervals, which were weighted according to the depth interval thickness (0.1 versus 0.2 m). This calculation was made for four soil profile depths, i.e., considering only part of the 0.0–3.0 m soil profile in order to obtain mean soil profile *SWC* values for three additional 'soil profile depths' of 0.0–0.5 m, 0.0–1.0 m, and 0.0–2.0 m.

During the *SWC* measurement period in Area A, gravimetric *SWC* was determined to a depth of 1.0 m in 0.1-m increments on seven occasions at 171 sample points along two transects on each side of the main gully of the Liudaogou watershed (Fig. 1). The seven *SWC* datasets were designated as *SWC*1, *SWC*2, *SWC*3, *SWC*4, *SWC*5, *SWC*6, and *SWC*7, corresponding to the samples collected for *SWC* determination on July 3–4, August 3–4, September 9–10, and October 17–18 in 2007, and on April 16–17, May 17–18, and June 20–21 in 2008, respectively. These dates were reasonably close (i.e., within a few days) to dates on which *SWC* measurements were carried out in Area A. Soil particle distribution, soil bulk density, saturated soil hydraulic conductivity, vegetation cover and topographic properties were determined for each of these additional sample points (She et al., 2013, 2014d) and for the locations P1–P20 in Area A. Volumetric *SWC* was computed from gravimetric *SWC* and soil bulk density values.

2.3. Statistical analysis

The 21 datasets of profile *SWC* in Area A were divided into a calibration set of 10 datasets (2007) and a validation set of 11 datasets (2008). The calibration datasets were used to identify the MTSL and MTSD from among the locations P1 to P20 based on computations of the MRD and standard deviation of relative difference (SDRD) of either the point-*SWC* relative to the areal-mean *SWC* (MTSL) or the depth-*SWC* relative to the mean soil profile *SWC* (MTSD) measurements. The validation datasets were used to verify that the MTSL and MTSD *SWC* values were applicable for upscaling to the scales of Area A as well as of the entire watershed.

To test the time stability concept for the MTSL, we used the indexes of MRD_L and $SDRD_L$ to represent their respective values in the lateral (i.e., the horizontal) direction across Area A, where the subscript L is used to denote the lateral direction. We defined three indices to the dimensions under investigation in these analyses, i.e., *i* refers to locations (P1–P20) across Area A, *j* refers to times of measurements made in Area A, and *k* refers to the depth intervals in the various soil profiles. In addition, *j* refers to times

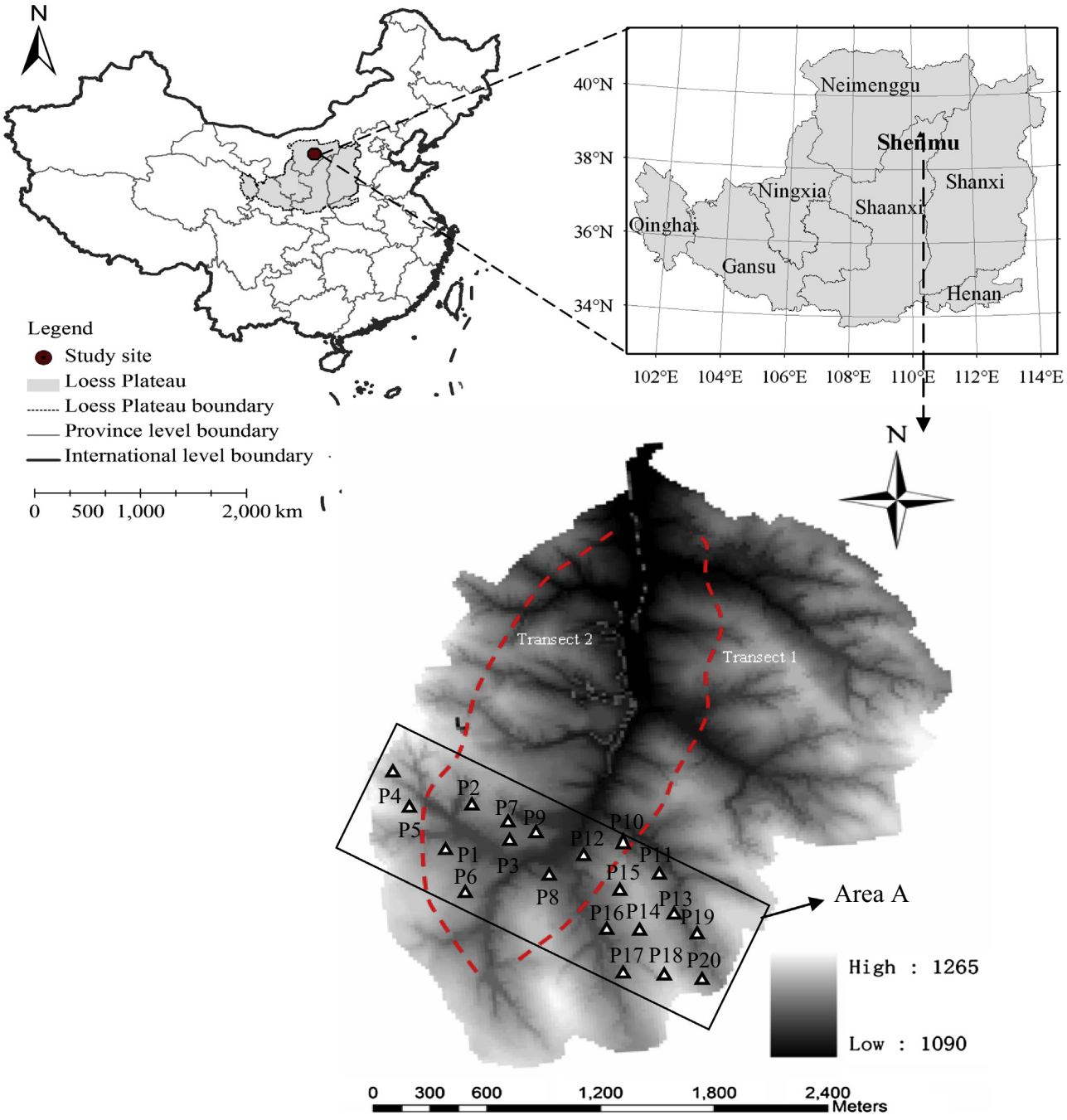

Fig. 1. Location of the Liudaogou watershed on the Chinese Loess Plateau, with the 20 designated measurement locations in Area A, and the additional sampled transects 1 and 2 to be used for comparison of soil water content time stability analysis results.

in the calibration period, while j' refers to times in the validation period. According to Vachaud et al. (1985), we defined δ_{ij} as the relative difference of *SWC* at location i measured at a time j, as compared with the areal-mean *SWC*:

$$\delta_{ij} = \frac{S_{ij} - \overline{S_j}}{\overline{S_j}} \tag{1}$$

where S_{ij} (%) is the mean soil profile *SWC* at location i measured at time j, and $\overline{S_j}$ is the spatial or areal-mean *SWC* (%) of Area A at the time j and can be expressed as $\overline{S_j} = \frac{1}{l}\sum_{i=1}^{l} S_{ij}$, where l refers to the number of sampling locations, i.e., $l = 20$ in this study. The mean relative difference, $\overline{\delta_i}$ was then computed by averaging the 10 relative differences, δ_{ij}, calculated for a given location, i, at the 10 measurement times. Using the mean relative difference, both the MRD_L and $SDRD_L$ were computed by:

$$\mathrm{MRD_L}(i) = \overline{\delta_i} = \frac{1}{m}\sum_{j=1}^{m}\delta_{ij} \tag{2}$$

and

$$\mathrm{SDRD_L}(i) = \sum_{j=1}^{m}\left(\frac{(\delta_{ij} - \overline{\delta_i})^2}{m-1}\right)^{1/2} \tag{3}$$

where m denotes the number of sampling times during the calibration period (2007, $m = 10$). For the subsequent validation period

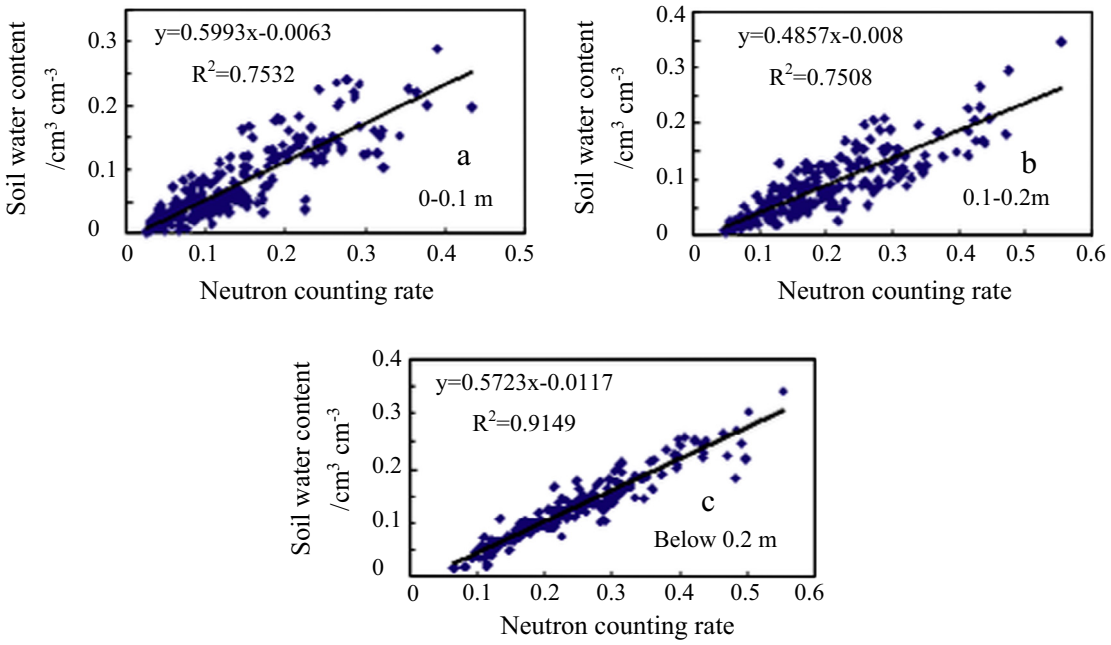

Fig. 2. Neutron probe calibration curves for the soil layers at depths of (a) 0.0–0.1 m, (b) 0.1–0.2 m and (c) below 0.2 m. R^2 is the coefficient of determination for the linearly regressed line passing among the data points. The regression equations and corresponding R^2-values indicate *SWC* uncertainty of about 0.05 $cm^3\ cm^{-3}$ for the near-surface measurements and about 0.03 $cm^3\ cm^{-3}$ for the measurements made in deeper soil layers.

(2008), the predicted areal-mean *SWC* of Area A ($\widehat{A}_{SL}$) at time j', $\widehat{S}_{j'}$, is obtained by:

$$\widehat{A}_{SL} = \widehat{S}_{j'} = \frac{1}{n}\sum_{i=1}^{n}\frac{S_{ij'}}{1+\overline{\delta_i}} \tag{4}$$

where n is the number of selected highest ranked time-stable locations (varies from 1 to 10), $\overline{\delta_i}$ is the MRD_L for the time-stable location i for the calibration period, and $S_{ij'}$ is the profile *SWC* measured at a time-stable location i at the time j' for each of the 11 measurement times during the validation period in 2008. Eq. (4) is based on the second method described by Grayson and Western (1998), which uses a constant offset term ($\overline{\delta_i}$), which in our case is the MRD_L. In a later analysis, we will compare these predicted areal-mean *SWC* values with the measured areal-mean values, $\overline{S_{j'}}$.

Analogous with Eqs. (1)–(4), we defined equivalent statistical parameters for the vertical or depth direction, replacing the subscript index, *L*, by *D*. As such, for each location, δ_{kj} now represents the relative difference of *SWC* at a depth k measured at a time j.

$$\delta_{kj} = \frac{S_{kj} - \overline{S_k}}{\overline{S_k}} \tag{5}$$

where S_{kj} is the *SWC* measured at a depth interval k (k = 1–5; 1–10; 1–15; or 1–20 for the four analyzed soil profile depths of 0.5, 1, 2, or 3 m, respectively) at the time j, while $\overline{S_k}$ is the mean soil profile *SWC* based on the averaged depth *SWC*, at a time, j, which can be expressed as $\overline{S_k} = \frac{1}{d}\sum_{k=1}^{d} S_{kj}$, i.e., it is averaged value of the *SWC* measured at each depth, k, within a soil profile that has d depth intervals (d = 5, 10, 15, 20 for the soil profile depths, respectively). This was calculated at each measured location, i, of the 20 Area A locations (P1–P20) measured at the time, j. The mean relative difference, $\overline{\delta_k}$, was then calculated for the 10 measurement times. The temporal MRD_D and $SDRD_D$ were given by:

$$MRD_D(k) = \overline{\delta_k} = \frac{1}{m}\sum_{j=1}^{m}\delta_{kj} \tag{6}$$

and

$$SDRD_D(k) = \sum_{j=1}^{m}\left(\frac{(\delta_{kj} - \overline{\delta_k})^2}{m-1}\right)^{1/2} \tag{7}$$

Hence, for the validation period (2008), the predicted mean soil profile *SWC* for each P-location at time j', $\widehat{S}_{ij'}$, is obtained from:

$$\widehat{S}_{ij'} = \frac{S'_{ij'}}{1+\overline{\delta_k}} \tag{8}$$

where $S'_{ij'}$ is the *SWC* measured at the MTSD in the measurement location i at time j' during the 2008 validation period.

Then, the predicted areal-mean *SWC* of Area A ($\widehat{A}_{SD}$) based on the MTSD *SWC* measurements at time j', $\widehat{S}_{j'}$, is obtained from:

$$\widehat{A}_{SD} = \widehat{S}_{j'} = \frac{1}{n}\sum_{i=1}^{n}\frac{\widehat{S}_{ij'}}{1+\overline{\delta_i}} \tag{9}$$

where $\overline{\delta_i}$ was obtained from the calibration period using Eq. (2), and n was the number of selected highest ranked time-stable locations. The term, $\widehat{S}_{ij'}$ is the mean soil profile *SWC* predicted by Eq. (8) at a time-stable location i at the time j'.

Intuitively, it should be clear that smaller values for $SDRD_L(i)$ or $SDRD_D(k)$ indicate the increasing probability of time stability for the specific location i or depth interval k. (Grayson and Western, 1998; She et al., 2012). Following the recommendations by Vachaud et al. (1985), we used a critical SDRD value of 10% to identify time-stable locations or depth intervals. The MTSL and MTSD were assigned to the respective location and depth interval with the minimum corresponding SDRD value.

The relative bias to the mean (*RBM*) was computed to assess the mean *SWC* prediction error for the test period, given as:

$$RBM = \frac{1}{q}\sum_{j'}^{q}\frac{|\widehat{S}_{j'} - \overline{S_{j'}}|}{\overline{S_{j'}}} \times 100 \tag{10}$$

where q = 11 and is the number of sampling times for the validation period; these calculations were performed to determine both the MTSLs and MTSDs. The Akaike information criterion (AIC_c) was used

to select the optimum number of stable locations based on the calculation of the residual sum of squares between observed and estimated values (Burnham and Anderson, 2002; Burnham et al., 2011), given by:

$$AICc = 2p + q\log\left[\sum(\widehat{S}_{j'} - \overline{S_{j'}})^2/q\right] + 2p(p+1)/(q-p-1) \quad (11)$$

where p is the number of time-stable locations.

In order to quantify the upscaling error, the independently-measured *SWC* dataset for the Liudaogou watershed scale (She et al., 2013, 2014c) was used to compare the area-representative *SWC* using the optimum number of MTSLs and MTSDs for Area A with the additional watershed-scale *SWC* measurements.

We compared the mean-measured *SWC* across the Liudaogou watershed with the estimated *SWC* using the time-stable locations (and depth intervals) for Area A, using the following equation (Parajka et al., 2005):

$$\widehat{S}^T_{j'} = S_{j'} \times r \quad (12)$$

where $\widehat{S}^T_{j'}$ is the estimated areal-mean *SWC* at time j' in the Liudaogou watershed, $\widehat{S}_{j'}$ is the predicted areal-mean *SWC* of Area A at time j' using Eqs. (4) or (9), and r is the ratio of the spatial mean *SWC* of Area A to that of the Liudaogou watershed.

3. Results and discussion

3.1. Temporal SWC patterns

Fig. 3a presents the vertical distribution of the temporal depth-mean *SWC*, i.e., the mean *SWC* of each soil depth within each soil profile derived from *SWC* measurements made at all 20 Area A locations (P1–P20) using depth *SWC* data collected for all 21 measurement times. From these graphs, we identified by observation four distinct vertical *SWC* patterns as a function of depth. These are patterns of (a) uniform *SWC* (e.g., P1, P20), (b) increasing *SWC* with depth (e.g., P18 and P19), (c) decreasing *SWC* with depth (e.g., P14 and P15), and (d) fluctuating with soil depth (e.g., P9 and P12). The distinct distributions are the combined result of water infiltration and soil evapotranspiration as determined by profile soil texture and land use (Heathman et al., 2003; She et al., 2014a), as well as by the presence of calcareous soil layers that impede soil water movement (Hu and Si, 2014). Specifically, based on past observations we found that the uniform *SWC* distribution pattern applies to measurement sites where there was shallow rooting vegetation, such as certain crops and natural grassland, and/or when the soil profile texture had higher clay contents, which may both have resulted in low plant evapotranspiration (ET); and/or where there was high soil water retention. The *SWC* patterns showing increasing *SWC* with depth are likely in coarse-texture soils, facilitating infiltration and redistribution to deeper soil layers. The *SWC* tended to decrease with soil depth under vegetation with high ET and deep roots, for example for *Caragana korshinskii* trees and alfalfa (*Medicago sativa*L.). The profiles with fluctuating *SWC* values with depth are likely the result of depth variations of plant root distributions and water redistribution caused by impeding calcareous soil layers. It should be noted that the effect of neutron escape, which may occur to a depth of 15 cm, might also have contributed to the profile distributions of *SWC* (Haverkamp et al., 1984). This might have contributed to the lower coefficients of determination obtained for the calibration curves for the two upper soil layers (Fig. 2a and b). However, the contribution of neutron escape did not appear to obscure the natural *SWC* distribution patterns.

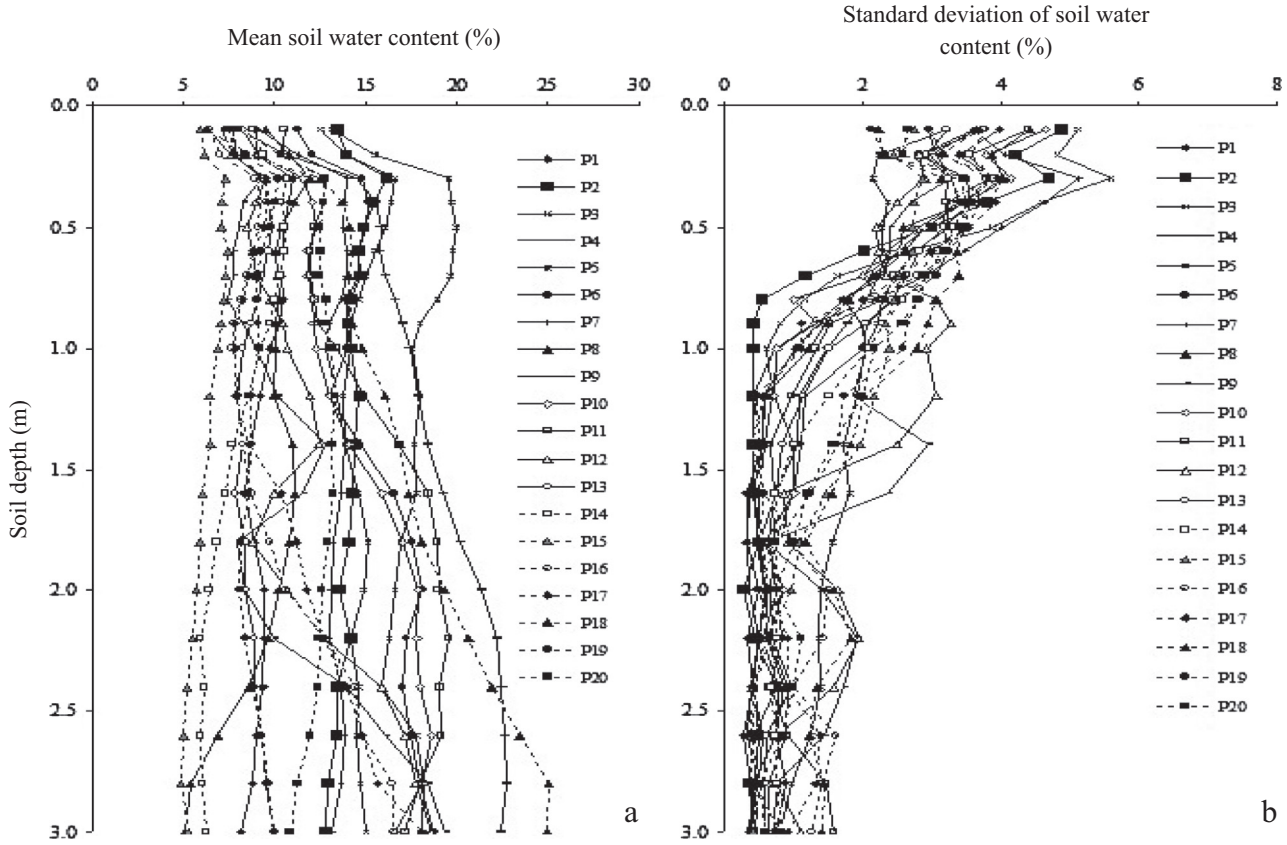

Fig. 3. (a) Mean volumetric soil water contents and (b) their standard deviations determined from measurements of the soil water content measured on 21 occasions at various soil depths and sampling locations in Area A.

The temporal variation of *SWC*, as computed by the standard deviation, typically decreased with increasing soil depth (Fig. 3b), especially for the 0–1.0 m soil depth. This agrees well with previous observations for various land use types and for a large range of time–space scales (Choi and Jacobs, 2007; Gao and Shao, 2012), although the total soil depth over which the decrease occurred varied among the studies. This *SWC* decrease, which manifests itself mostly for the near soil surface layer, is caused largely by decreases in root water uptake (Hupet and Vanclooster, 2002) with increasing depth and/or by soil evaporation (Hu et al., 2010), which mostly occurs from soil water stored in the top soil. The combined effects of evaporation and transpiration loses, which

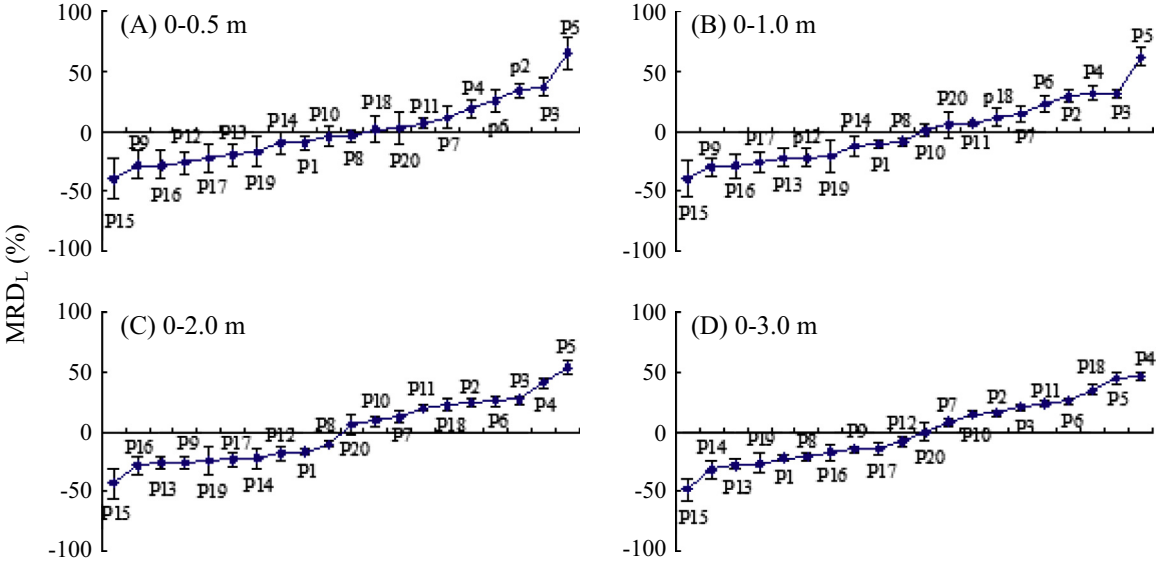

Fig. 4. Ranked mean relative difference (MRD$_L$) of profile-mean soil water content (*SWC*) for each soil profile depths of (A) 0–0.5 m, (B) 0–1.0 m, (C) 0–2.0 m and (D) 0–3.0 m. Bars represent the standard deviation of relative difference (SDRD$_L$) for 20 measurement locations (P1–P20) in Area A.

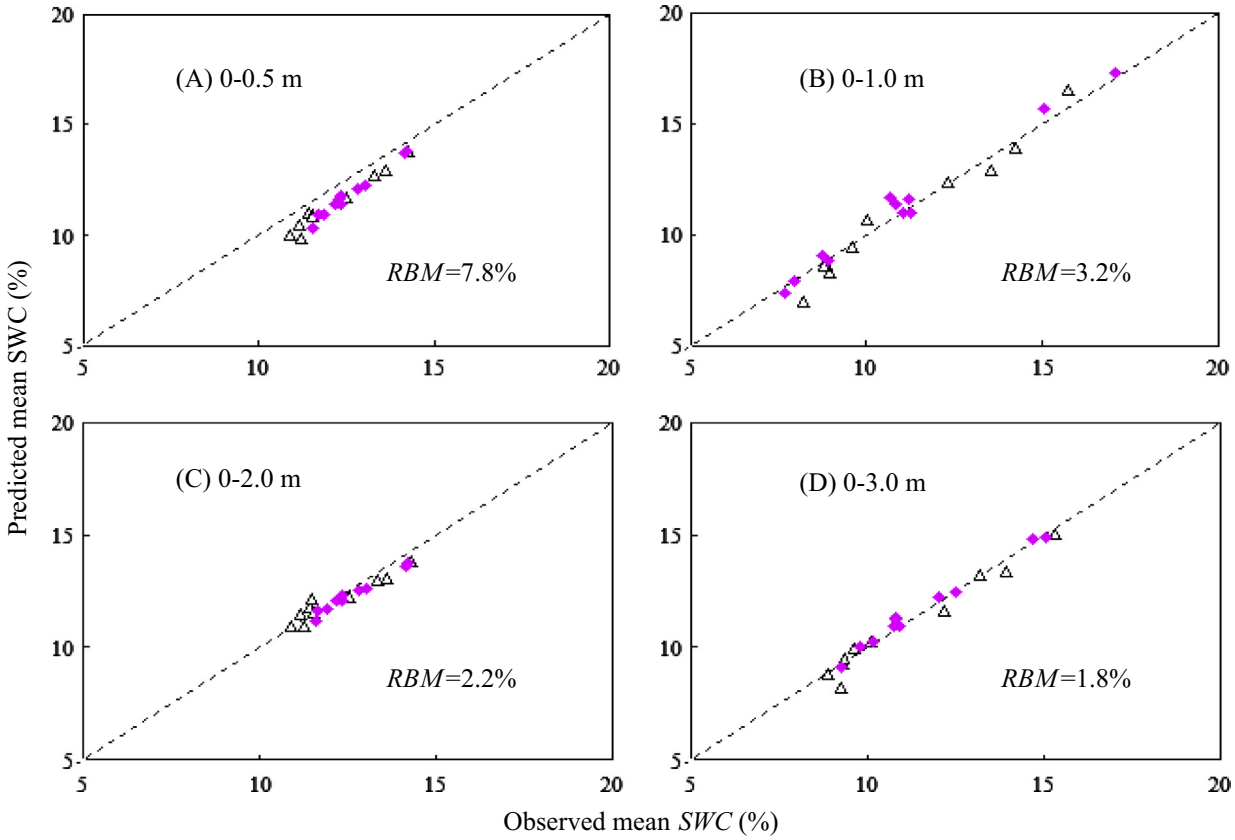

Fig. 5. Predicted versus observed areal-mean soil water contents (*SWC*) in Area A for both the calibration (triangle) and validation (diamonds) periods for soil profile depths of (A) 0.5 m, (B) 1.0 m, (C) 2.0 m and (D) 3.0 m. The predicted areal-mean *SWC* ($\hat{A}_{SL}$) was obtained by using *SWC* measurements in the soil profiles at the most-time-stable-location i.e., at P11 alone.

are both depth dependent, results in the dominance of ET on the depth distribution of *SWC* and are likely important factors that ensure time stability (She et al., 2014a).

3.2. Time stability analysis – locations

Fig. 4 presents the rank-ordered MRD_L with associated $SDRD_L$ values for the mean soil profile *SWC* at each location (P1–P20) in Area A, as computed using Eqs. (2) and (3) from the 10 measurement times of the calibration period. The range in MRD_L values (computed as the maximum value – the minimum value) decreased from 105% for the 0.5-m deep soil profile (Fig. 4A), to 102%, 98% and 96% for the 1.0-, 2.0-, and 3.0-m deep soil profiles (Fig. 4B–D), respectively. This indicated that *SWC* spatial variability was reduced as the soil profile depth increased, albeit only slightly. The lowest MRD_L value was observed for location P15, signifying its *SWC* was the lowest, relative to its field-mean. This was likely caused by the high sand content (69.3%) in the upper 0.2-m layer of P15 as compared with the Area-mean value (36.8%). Maximum values of MRD_L values were determined for those locations in cropland and bare soil (e.g., locations P5 and P4), which were characterized by relatively low ET rates when compared with other locations in the study area. Locations with higher ET rates included those under crops growing in soils with lower clay contents and those under vegetation that had higher transpiration rates, e.g., alfalfa and caragana (She et al., 2014b). Measurement locations with

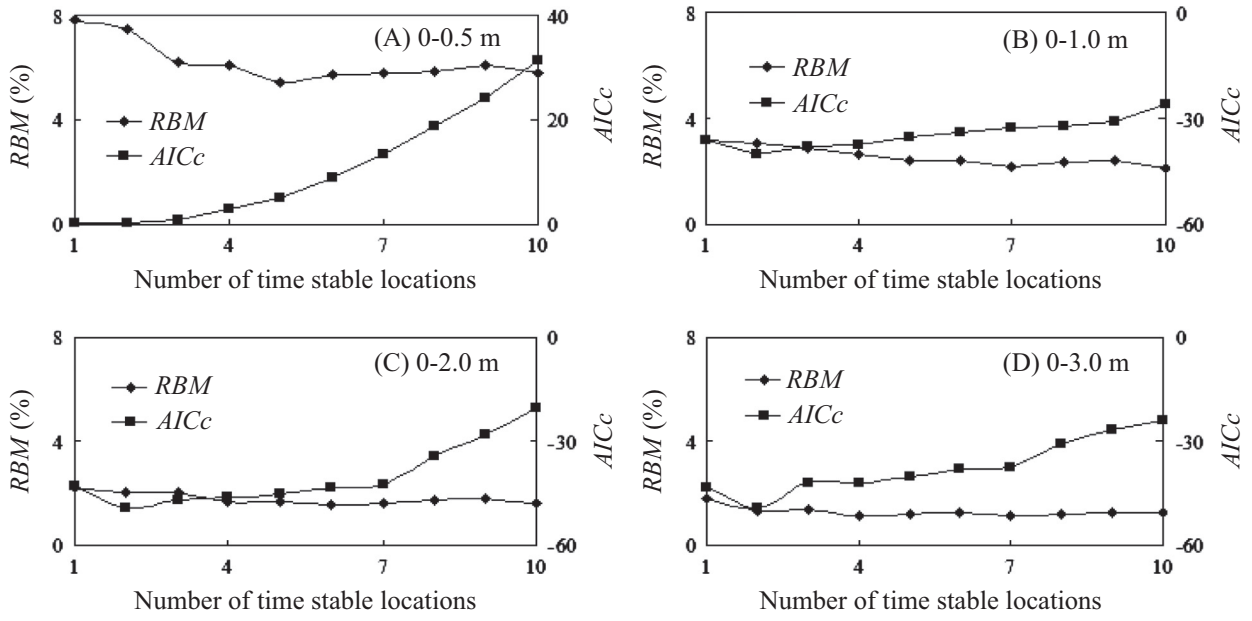

Fig. 6. Relative bias to the mean (*RBM*) soil water content (*SWC*) and the Akaike information criterion (*AICc*) for areal-mean *SWC* estimations made for Area A ($\hat{A}_{SL}$) for soil profile depths of (A) 0.5 m, (B) 1.0 m, (C) 2.0 m and (D) 3.0 m. The estimations used different numbers of the most highly-ranked time-stable-locations.

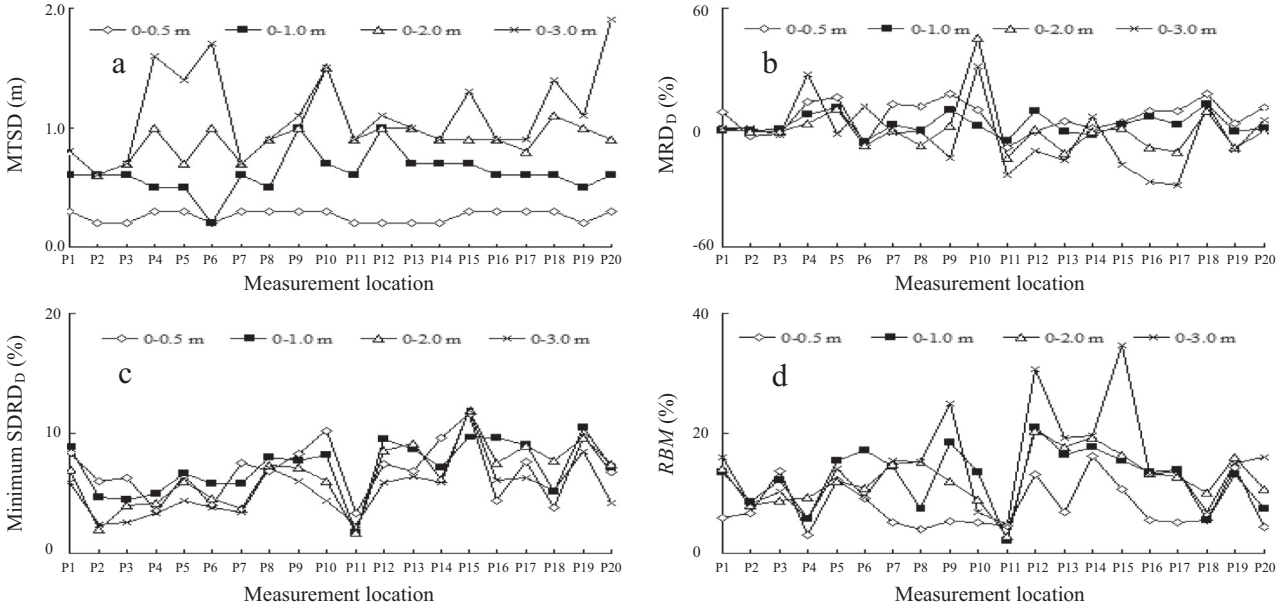

Fig. 7. (a) The most time-stable depth (MTSD) and associated (b) mean relative difference (MRD_D), (c) minimum standard deviation of relative difference ($SDRD_D$), and (d) relative bias to the mean (*RBM*) soil water contents (*SWC*) of soil profile depths of 0.5, 1.0, 2.0, and 3.0 m for 20 *SWC* measurement locations.

MRD-values near zero are represented by the cluster of locations P1, P7, P8, P10, P11, P18 and P20, thus being the closest to the field-mean *SWC*.

The $SDRD_L$ value of the mean soil profile *SWC* provides us with an indicator of the level of time stability. For example, values of $SDRD_L$ for the 0.5 m top soil profile (Fig. 4A) ranged between 3.8% and 17.2%, with 12 of the 20 measurement locations having $SDRD_L$ values lower than 10%. An SDRD value of 10% was defined by Vachaud et al. (1985) as the cut-off value separating time-stable from unstable measurement locations. The $SDRD_L$ values

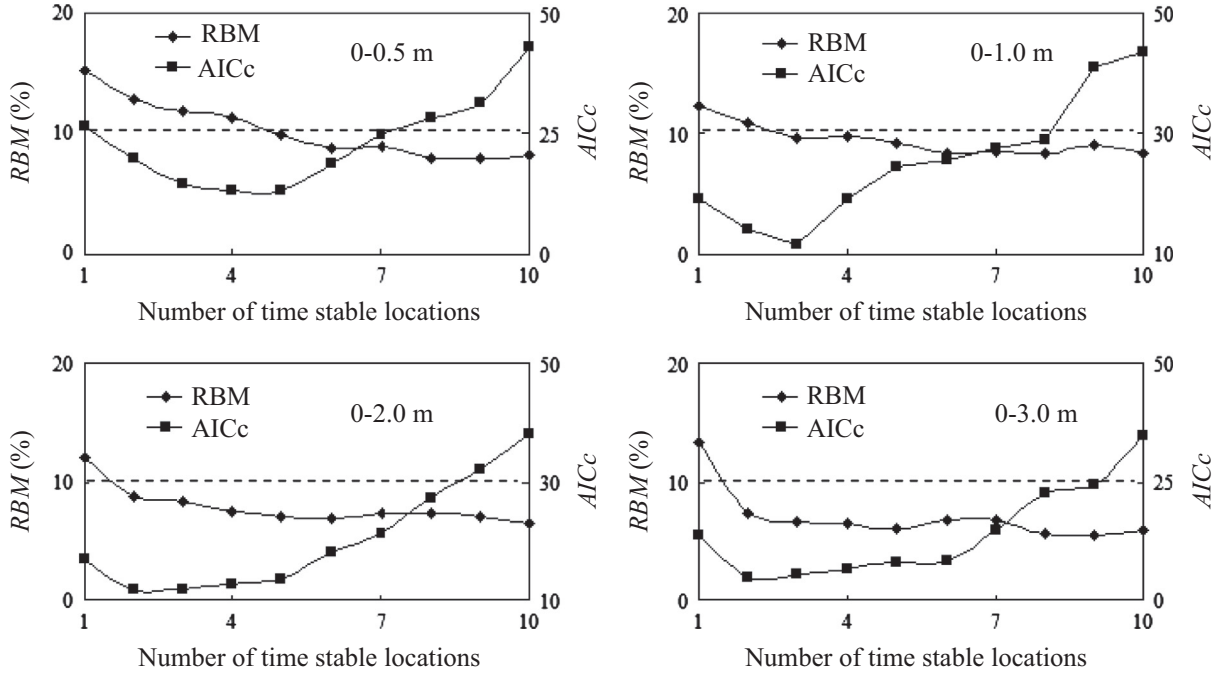

Fig. 8. Relative bias to the mean (*RBM*) soil water content (*SWC*) and the Akaike information criterion (*AICc*) obtained when estimating the areal-mean *SWC* ($\widehat{A}_{SD}$) using the measured *SWC* at the most-time-stable-depth in different numbers of the most highly-ranked time-stable-locations.

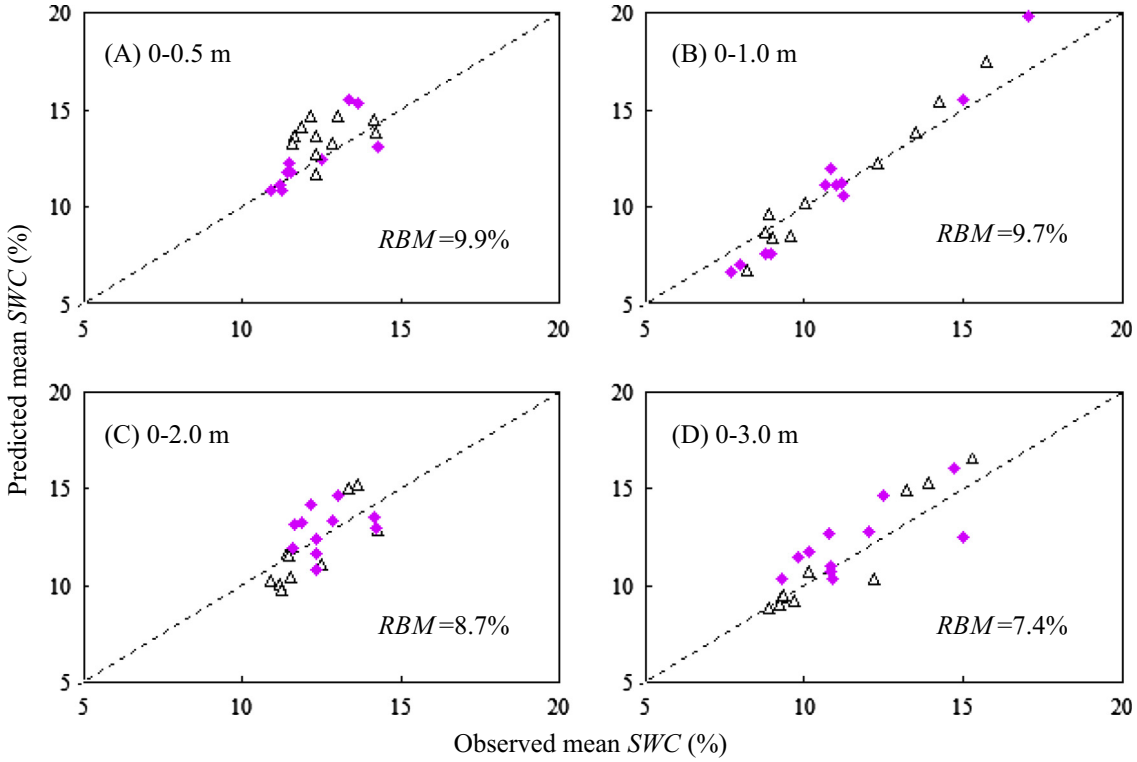

Fig. 9. Predicted versus observed areal-mean soil water content (*SWC*) for Area A for both the calibration (triangle) and validation (diamonds) periods for four soil profile depths. The predicted areal-mean *SWC* ($\widehat{A}_{SD}$) was acquired by using the *SWC* measurements made at the most-time-stable-depths of the optimum number of more highly ranked time-stable-locations. *RBM* is the relative bias to the mean *SWC*.

decreased with increasing soil profile depth, with about 85%, 90% and 100% of locations within Area A identified as time-stable locations for profile depths of 1.0, 2.0, and 3.0 m, respectively. The MTSL, corresponding to the minimum $SDRD_L$ value, was location P11 for all four soil profile depths (Fig. 4).

To evaluate the potential of using the MTSL to represent area-wide *SWC*, we applied Eq. (4) with $n = 1$, using only P11 as the MTSL. This was done for both the calibration (triangle) and validation (diamonds) periods (Fig. 5). Furthermore, we performed this calculation for the four soil profile depths, i.e., 0–0.5 cm, 0–1.0 cm, 0–2.0 m and 0–3.0 m. The predicted $\widehat{A}_{SL}$ was in agreement with the observed *SWC* for all four soil profiles with *RBM* values as computed from Eq. (10) of 7.9%, 3.2%, 2.2% and 1.8%. Therefore, we concluded that the prediction accuracy of using the MTSL was larger as the soil profile depth increased, and is consistent with the time stability analysis of Fig. 4. As all *RMB* values were smaller than 10%, we concluded that using only one MTSL was sufficiently accurate to estimate the areal-mean *SWC* for Area A.

To evaluate the *SWC* accuracy by including additional MTSLs in Eqs. (4) and (10), values of *RBM* were plotted as a function of the number of MTSLs in order of rank in Fig. 6. As would be expected, *RBM* decreased as the number of MTSLs is increased. However, this was only the case for the 0.5 and 1.0 m soil profiles (Fig. 6A and B), whereas *RBM* was mostly independent of the number of MTSLs for the larger depth intervals. We note that the increasing number of measurement locations requires larger expenditures of labor, time, and resources in general, thereby offsetting the gain in accuracy (Jia and Shao, 2013). Since minimum values of *AICc*, calculated by Eq. (11), were very close whether using one or two top-ranked stable locations, we concluded that measuring the profile *SWC* at just a single time-stable location would be adequate for estimating $\widehat{A}_{SL}$ for all of the four evaluated soil profile depths.

3.3. Time stability analysis – soil depth intervals

In the following, we analyzed the MTSD interval that would represent the soil profile mean *SWC*. This was done for each of the 20 measurement locations and four soil profile depths. The MTSD was identified as the measured depth interval with the minimum $SDRD_D$ value. The MTSD (Fig. 7A), and associated MRD_D (Fig. 7B), $SDRD_D$ (Fig. 7C), and estimation error (*RBM*) values (Fig. 7D) varied with soil profile depth and location. Mean values of the MTSD were computed for the 20 locations (P1–P20) (Fig. 7A), and were equal to 0.3, 0.6, 0.9, and 1.1 m for soil profile depths of 0.5, 1.0, 2.0, and 3.0 m, respectively. Hence, the MTSDs were all approximately located halfway down any given soil profile. Some of the *RBM* values used to evaluate the accuracy of soil profile mean *SWC* prediction from the MTSD data of *SWC* were larger than 10% (but most were still less than 20%), even though the minimum $SDRD_D$ values were less than 10% for the majority of sampling locations of the evaluated soil profiles. Much of the higher *RBM* values were due to the *SWC* data being collected with large intervals between measurement times, thereby decreasing time stability of the vertical *SWC* patterns (She et al., 2012; Hu and Si, 2014). We note that the MTSL P11 was identified as the optimum location for which the mean soil profile *SWC* was most reliably predicted from the MTSD with a *RBM* value of less than 5% (Fig. 7D) and a minimum $SDRD_D$ of 3% (Fig. 7C). Other locations with low *RBM* values were P4, P18 and P20.

In order to determine the optimum number of MTSLs to be used with the MTSD values in order to predict the areal-mean *SWC* of Area A ($\widehat{A}_{SD}$), we analyzed the distribution of *RBM* values as shown in Fig. 8 for all four soil profile depths. We note that by selecting only a single depth increment, the estimation error of $\widehat{A}_{SD}$ (or *RBM)* was typically larger than by using the MTSLs ($\widehat{A}_{SL}$) (Fig. 6). When using only the single MTSD (0.2, 0.6, 0.9, and 0.9 m for soil profile depths of 0.5, 1.0, 2.0, and 3.0 m, respectively) at the MTSL (P11), *RBM* values were all higher than 10% (Number of time-stable locations is 1, in Fig. 8). Our results suggested that the estimation error decreased if additional highly-ranked MTSLs were included in the analysis (Fig. 8). For example, for the 0.5-m soil profile analysis, *RBM* values decreased to less than 10% when the first five top-ranked MTSLs were included when estimating $\widehat{A}_{SD}$ using Eq. (9). We note that our analysis clarified that the location-specific MTSD in Fig. 7A should be used for each of the highest-ranked MTSLs. In order to achieve *RBM* values <10% and get the lowest *AICc* values, required that the MTSD *SWC* measurements should be made at the 5 (for the 0.5-m soil profile), 3 (1.0-m soil profile), and 2 (for

Table 1
Comparison of Relative Bias to the Mean (*RBM*) *SWC* values, when using the most time-stable location (MTSL) and the most time-stable depth (MTSD) in Area A to predict the areal-mean *SWC* of the Liudaogou watershed.

Measurement date in Liudaogou watershed	Using MTSL		Using MTSD of MTSLs	
	0–0.5 m	0–1.0 m	0–0.5 m	0–1.0 m
July 3, 2007	8.97	8.55	11.09	8.62
August 3, 2007	9.22	5.52	12.73	9.49
September 9, 2007	7.08	5.47	12.51	7.58
October 17, 2007	8.60	6.97	13.97	9.73
April 16, 2008	5.28	5.78	11.56	7.28
May 17, 2008	6.52	7.47	11.04	7.31
June 20, 2008	9.45	6.16	11.21	8.88
[a]All	4.89	5.69	11.83	7.10

[a] The time-averaged ratio of the areal-mean soil water content (*SWC*) at the two scales was taken as the slope of the linear regression equation (Fig. 10) relating the areal-mean *SWC* of the Liudaogou watershed to that of Area A for the seven measurement dates.

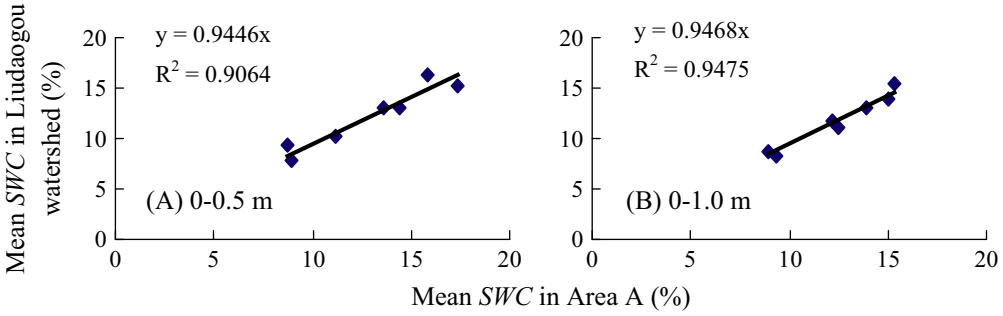

Fig. 10. Comparison of the mean soil water content (*SWC*) of the Liudaogou watershed with the mean *SWC* of Area A, for soil profile depths of (A) 0.5 m and (B) 1.0 m. R^2 is the coefficient of determination for the linearly regressed line passing among the data points.

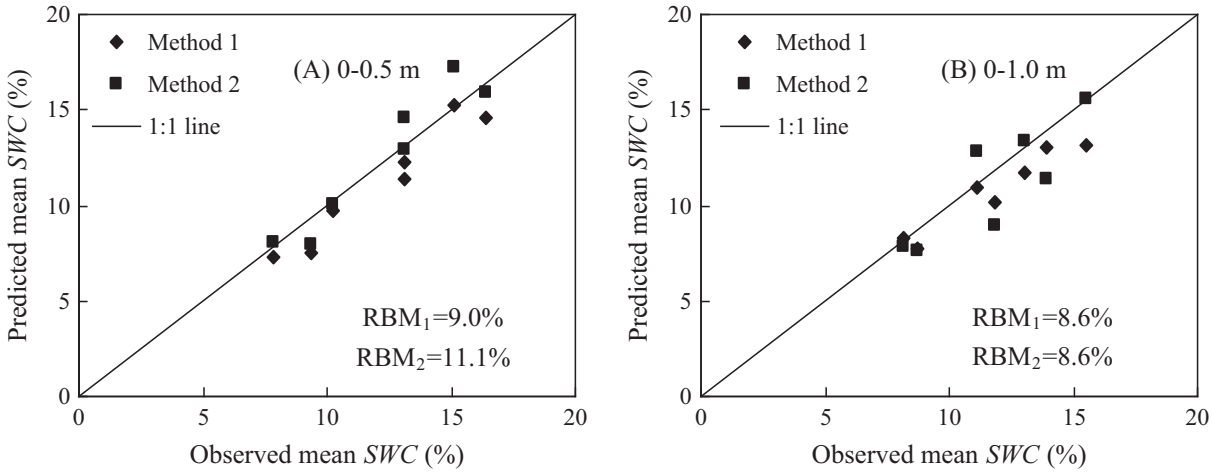

Fig. 11. Predicted versus observed mean soil water contents (*SWC*) in the soil profile depths of (A) 0.5 m and (B) 1.0 m at the Liudaogou watershed scale. The graphs compare Method 1, which used the most-time-stable-location (MTSL), with Method 2, which used the most-time-stable-depth at the most highly ranked MTSLs. *RBM* is the relative bias to the mean *SWC*.

both the 2.0- and 3.0-m soil profiles) highest-ranked MTSLs (Fig. 8). The corresponding comparison of predicted and observed areal-mean *SWC* values for Area A is presented in Fig. 9, for both the calibration and validation periods.

3.4. Upscaling of SWC

Finally, it was proposed to apply the time stability concept to the upscaling of the areal-mean *SWC* in Area A to the Liudaogou watershed. For that purpose, we corrected upscaled *SWC* by a time-invariable ratio (r) of the areal-mean *SWC* at the two measurement scales (Parajka et al., 2005). Parallel *SWC* measurements at both spatial scales were limited to 7 measurement times and to the upper 1.0-m soil profile depth. The comparison of measured *SWC* values for both areas are presented in Fig. 10, with R^2 values of 0.90 and 0.95 and zero intercepts for the 0.5-m and 1.0-m soil profile depths, respectively. Our results indicated that there was the potential of using *SWC* measurements at the MTSDs of the MTSL in Area A to estimate the watershed-mean *SWC* (Parajka et al., 2005; Hu et al., 2010), thereby greatly reducing the total number of required *SWC* measurements once a calibration had been established.

In order to evaluate this approach, we predicted the areal-mean *SWC* of the Liudaogou watershed, using Eq. (12), and both the estimated areal-mean *SWC* of Area A acquired by either using the MTSL ($\widehat{A}_{SL}$, Method 1) or the MTSD ($\widehat{A}_{SD}$, Method 2) for identical sampling dates. The results are presented in Table 1 and compared in Fig. 11 for all 7 measurement times and for two soil profile depths. For Method 1, we used profile *SWC* measurements for the MTSL (location P11 only). For Method 2, we used only the MTSD measurements of *SWC* for the five (0.5-m soil profile) and three (1.0-m soil profile) highest-ranked MTSLs. Taking the ratio of the mean *SWC* on the first date (July 3, 2007), for example, predicted mean *SWC* values close to those measured for both the 0.5-m (Fig. 11A) and 1.0-m soil profile depths (Fig. 11B). In Table 1, we compare the *RBM* values obtained using both the time-specific and the time-averaged r-values (bottom row). We note that the upscaled *SWC* estimations were better for the 1.0- than for the 0.5-m soil profile depth. This was indicated by the larger *SWC* estimation errors obtained when using the presented time-stability analysis for the shallower soil profile as well as by the lower R^2 values acquired when comparing the mean *SWC*s of Area A and the watershed (Fig. 10).

4. Conclusions

We evaluated the use of time stability analysis to estimated areal-mean soil water content (*SWC*) using the Most Time Stable Location (MTSL) as well as applying the concept to the Most Time Stable Depth interval (MTSD) for each of an optimum number of MTSLs. Once such an analysis is conducted for a calibration period, the number of required *SWC* measurement locations can be greatly reduced for subsequent long-term measurements.

When limiting profile *SWC* measurements to the MTSL (P11 only), the areal-mean *SWC* of Area A for the 0.5-, 1.0-, 2.0-, and 3.0-m soil profiles could be predicted with a relative error of less than 10% of the areal-mean *SWC*. Using the MTSLs, the Most Time-Stable Depth intervals were largely identified at the midway positions down the four examined soil profiles of 0.5, 1.0, 2.0 and 3.0 m. The most accurate estimated areal-mean *SWC* for Area A was obtained by using the MTSD at the MTSL (P11). However, additional MTSLs were required to determine the areal-mean *SWC* with an estimation error of less than 10%. The same identified MTSLs and MTSDs were successfully used to upscale to the watershed-scale mean *SWC*. Our results strongly indicated that time stability analysis could greatly reduce the required number of sampling locations and soil depths in arid and semi-arid climates, if area-representative *SWC* values should be needed, such as for water balance calculations.

Acknowledgements

We acknowledge and are grateful for the financial support provided by the National Natural Science Foundation of China through Grant No. 41471180 – China, the Excellent Creative Talents Support Program of Hohai University – China, and the Open Funding Project (No. Y412201423) of the State Key Laboratory of Soil and Sustainable Agriculture (Institute of Soil Science, Chinese Academy of Sciences) – China, and the Fundamental Research Funds for the Central Universities (2015B14814) – China, and by China Scholarship Council – China.

References

Brocca, L., Melone, F., Moramarco, T., Morbidelli, R., 2008. Soil moisture temporal stability over experimental areas in Central Italy. Geoderma 148, 364–374.
Burnham, K.P., Anderson, D.R., 2002. Model Selection and Multimodel Inference: A Practical Information-Theoretic Approach, second ed. Springer-Verlag, New York.

Burnham, K.P., Anderson, D.R., Huyvaert, K.P., 2011. AIC model selection and multimodel inference in behavioral ecology: some background, observations, and comparisons. Behav. Ecol. Sociobiol. 65, 23–35.
Choi, M., Jacobs, J.M., 2007. Soil moisture variability of root zone profiles within SMEX02 remote sensing footprints. Adv. Water Resour. 30, 883–896.
Corradini, C., 2014. Determination of soil moisture: measurements and theoretical approaches. J. Hydrol. 516, 1–5.
FAO/UNESCO, 1988. Soil Map of the World. Revised Legend. FAO/UNESCO, Rome.
Gao, L., Shao, M.A., 2012. Temporal stability of soil water storage in diverse soil layers. Catena 95, 24–32.
Gao, X., Wu, P., Zhao, X., Zhou, X., Zhang, B., Shi, Y., Wang, J., 2013. Estimating soil moisture in gullies from adjacent upland measurements through different observation operators. J. Hydrol. 486, 420–429.
Gómez-Plaza, A., Alvarez-Rogel, J., Albaladejo, J., Castillo, V., 2000. Spatial patterns and temporal stability of soil moisture across a range of scales in a semiarid environment. Hydrol. Process. 14, 1261–1277.
Grayson, R.B., Western, A.W., 1998. Towards areal estimation of soil water content from point measurements: time and space stability of mean response. J. Hydrol. 201 (1–2), 68–82.
Haverkamp, R., Vauclin, M., Vachaud, G., 1984. Error analysis in estimating soil water content from neutron probe measurements: 1. Local standpoint. Soil Sci. 137, 78–90.
Heathman, G.C., Starks, P.J., Ahuja, L.R., Jackson, T.J., 2003. Assimilation of surface soil moisture to estimate profile soil water content. J. Hydrol. 207, 42–55.
Hu, W., Shao, M.A., Han, F.P., Reichardt, K., Tan, J., 2010. Watershed scale temporal stability of soil water content. Geoderma 158, 181–198.
Hu, W., Si, B.C., 2014. Can soil water measurements at a certain depth be used to estimate mean soil water content of a soil profile at a point or at a hillslope scale? J. Hydrol. 516, 67–75.
Hu, W., Tallon, L.K., Si, B.C., 2012. Evaluation of time stability indices for soil water storage upscaling. J. Hydrol. 475, 229–241.
Hupet, F., Vanclooster, M., 2002. Intraseasonal dynamics of soil moisture variability within a small agricultural maize cropped field. J. Hydrol. 261, 86–101.
Jia, Y.H., Shao, M.A., 2013. Temporal stability of soil water storage under four types of revegetation on the northern Loess Plateau of China. Agric. Water Manag. 117, 33–42.
Liu, B., Shao, M., 2014. Estimation of soil water storage using temporal stability in four land uses over 10 years on the Loess Plateau, China. J. Hydrol. 516, 974–984.
Mohanty, B.P., Skaggs, T.H., 2001. Spatio-temporal evolution and time-stable characteristics of soil moisture within remote sensing footprints with varying soil, slope, and vegetation. Adv. Water Resour. 24, 1051–1067.
Molina, A.J., Latron, J., Rubio, C.M., Gallart, F., Llorens, P., 2014. Spatio-temporal variability of soil water content on the local scale in a Mediterranean mountain area (Vallcebre, North Eastern Spain). How different spatio-temporal scales reflect mean soil water content. J. Hydrol. 516, 182–192.
National Geographic Society, 2010. Water: Our thirsty world – A Special Issue. National Geographic, April.
Parajka, J., Scipal, K., Komma, J., Blöschl, G., Wagner, W., Kidd, R., Bartalis, Z., Naeimi, V., 2005. Spatial and temporal dynamics of soil moisture in ungauged basins. Interim Report, Hydrology of Austria Programme (HÖ), Austrian Academy of Sciences.
Rolston, D.E., Biggar, J.W., Nightingale, H.I., 1991. Temporal persistence of spatial soil water patterns under trickle irrigation. Irrig. Sci. 12, 181–186.
She, D.L., Liu, D.D., Liu, Y.Y., Liu, Y., Xu, C.L., Qu, X., Chen, F., 2014a. Profile characteristics of temporal stability of soil water storage in two land uses. Arab. J. Geosci. 7, 21–34.
She, D.L., Liu, D.D., Xia, Y.Q., Shao, M.A., 2014b. Modeling effects of land use and vegetation density on soil water dynamics: implications on water resource management. Water Resour. Manage 28, 2063–2076.
She, D.L., Liu, D.D., Peng, S.Z., Shao, M.A., 2013. Multi-scale influences of soil factors on soil water content distribution in a watershed on the Chinese Loess Plateau. Soil Sci. 178 (10), 530–539.
She, D.L., Liu, Y.Y., Shao, M.A., Timm, L.C., Yu, S.E., 2012. Temporal stability of soil water content for a shallow and deep soil profile at a small catchment scale. Aust. J. Crop Sci. 6 (7), 1192–1198.
She, D.L., Shao, M.A., Timm, L.C., et al., 2010. Impacts of land use pattern on soil water content variability in the Loess Plateau of China. Acta Agric. Scand. Sect. B – Soil Plant Sci. 60, 369–380.
She, D.L., Tang, S.Q., Shao, M.A., Yu, S.E., Xia, Y.Q., 2014c. Characterizing scale specific depth persistence of soil water content along two landscape transects. J. Hydrol. 519, 1149–1161.
She, D.L., Zheng, J.X., Shao, M.A., Timm, L.C., Xia, Y.Q., 2014d. Scale specific relationships between saturated hydraulic conductivity and basic soil physical properties in two landscape transects. Clean – Soil, Air, Water. http://dx.doi.org/10.1002/clen.201400143.
Vachaud, G., Passerat de Silans, A., Balabanis, P., Vauclin, M., 1985. Temporal stability of spatially measured soil water probability density function. Soil Sci. Soc. Am. J. 49, 822–827.
Vereecken, H., Huisman, J.A., Bogena, H., Vanderborght, J., Vrugt, J.A., Hopmans, J.W., 2008. On the value of soil moisture measurements in vadose zone hydrology: a review. Water Resour. Res. 44, W00D06. http://dx.doi.org/10.1029/2008WR006829.
Vereecken, H., Huisman, J.A., Pachepsky, Y., Montzka, C., van der Kruk, J., Bogena, H., Weihermüller, L., Herbst, M., Martinez, G., Vanderborght, J., 2014. On the spatio-temporal dynamics of soil moisture at the field scale. J. Hydrol. 516, 76–96.
Xia, Y.Q., She, D.L., Li, Y.F., Yan, X.Y., 2014. Impact of sampling time on chamber-based measurements of riverine nitrous oxide emissions using relative difference analysis. Geoderma 214–215, 197–203.
Zucco, G., Brocca, L., Moramarco, T., Morbidelli, R., 2014. Influence of land use on soil moisture spatial–temporal variability and monitoring. J. Hydrol. 516, 193–199.